Reduced Equations for Rotationally Constrained Convection

Keith Julien
Department of Applied Mathematics, University of Colorado, Boulder, CO 80309-0526, USA

Edgar Knobloch
Department of Physics, University of California, Berkeley, CA 94720, USA

Joseph Werne
Colorado Research Associates, 3380 Mitchell Lane, Boulder, CO 80301, USA

ABSTRACT

The incompressible and anelastic Navier-Stokes equations are considered in the limit of rapid rotation (small Ekman number). The analysis is limited to horizontal scales small enough so that both horizontal and vertical velocities are comparable, but the horizontal velocity components are still in geostrophic balance. Asymptotic analysis leads to a pair of nonlinear equations for the vertical velocity and vertical vorticity coupled by vertical stretching. Statistically stationary states are maintained against viscous dissipation by thermal forcing. Direct numerical simulation of the reduced equations reveals the presence of intense vortical structures spanning the layer depth, in excellent agreement with recent experiments of Sakai (1997) and simulations of the Boussinesq equations for rotating convection by Julien, Legg, McWilliams & Werne (1996). Exact but fully nonlinear steady and oscillatory solutions of the reduced partial differential equations are found for various two- and three-dimensional planforms.

INTRODUCTION

Rotation-dominated turbulent convection is present in the oceans and atmosphere of the Earth, and in solar and giant planetary interiors. With these applications in mind the last few years have seen increased interest in the dynamics of rapidly rotating flows. However, flow characterization via observations is both costly and challenging. Laboratory experiments and numerical simulations therefore provide a valuable arena where rapidly rotating fluid flows can be investigated and appropriate theories developed. In this regard, rapidly rotating flows are generally believed to be simpler to understand because the strong rotation reduces the effective dimensionality of the system. The classical statement of this tendency is provided by the Taylor-Proudman theorem which asserts that, under appropriate conditions, rapid rotation confines any motion to two-dimensional planes orthogonal to the rotation axis (hereafter the z axis). Many flows in nature manifest this property, e.g. the large-scale motions of the Earth's atmosphere, and giant planet features such as the Great Red Spot of Jupiter. For these cases where horizontal scales are (or are believed to be) much greater than the vertical scales, reduced PDE descriptions of the Navier-Stokes equation have been derived. These include the shallow water, quasi-geostrophic, and balanced models (Pedlosky 1979, Gent and McWilliams 1983) and the recent $2+\epsilon$–dimensional turbulence models of Babin et al. (1997) and Majda & Embid (1997).

The presence of baroclinicity due to strong buoyancy forcing and of viscosity violates the basic assumptions of the Taylor-Proudman theorem, and generates flows parallel to the rotation axis. Such flows typically occur on near dissipative scales where the Taylor-Proudman constraint is easily relaxed. Despite these complications, the Taylor-Proudman theorem indicates that motion along the rotation axis will be inhibited for sufficiently rapid rotation, and suggests that the selected scales will be anisotropic, with the horizontal scales much smaller that the vertical scales. Indeed, recent visualization of laboratory convection by Sakai (1997) reveals the presence of tall Taylor-like columns. Sakai notes, however, that in his experiments the flow structure remains three-dimensional since the velocity field is isotropic. In the following, we show that despite this apparent three-dimensionality it is possible to capture the dynamics of rapidly rotating convection with a reduced set of partial differential equations. Like the $2+\epsilon$–dimensional equations mentioned above, these equations are derived using techniques that exploit the anisotropy in the horizontal and vertical scales.

In the following we summarize the derivation of the reduced PDEs for both incompressible and anelastic convection.

INCOMPRESSIBLE CONVECTION

The dimensionless Boussinesq equations describing incompressible convection in a horizontal fluid layer of depth

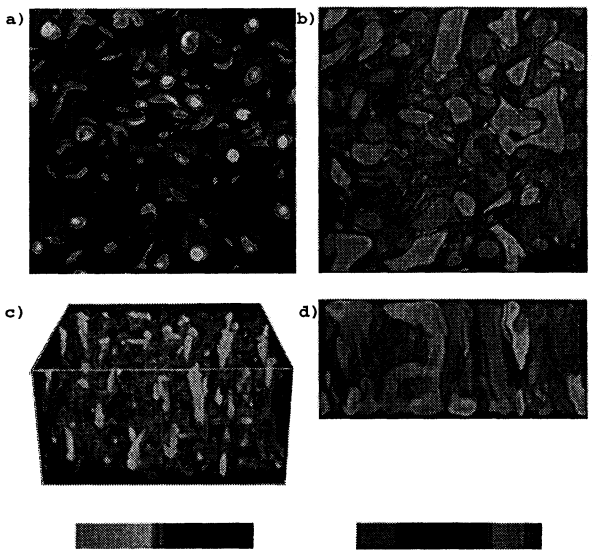

Figure 1: Results of direct numerical simulations of three-dimensional Boussinesq convection in the rapidly rotating regime (Julien et al. 1996). The visualization of vortical structures in (a,c) is in terms of the quantity λ_2 suggested by Jeong & Hussain (1995), where λ_2 is the intermediate eigenvalue of R^2+S^2, where R and S are, respectively, the rotation and strain matrices of the velocity field. The fluctuation temperature field θ is shown in (b,d). Plots (a,b) are top views, (c) perspective, and (d) sideview. The parameter values are Ra=1.0×10^7, E=9.4×10^{-5}, Ro=0.3, σ=1; the aspect ratio is 2×2×1 with periodic boundary conditions in the horizontal and stress-free conditions on the top and bottom boundaries. The simulation reveals the presence of slender coherent structures that span the depth of the layer. These structures are noticeably thinner in the λ_2 visualization than in the temperature field.

d rotating uniformly about the vertical are

$$\tfrac{1}{\sigma}\tfrac{D\mathbf{u}}{Dt}+\hat{\mathbf{z}}\times\mathbf{u}=-\nabla\pi+RaE^2\,T\hat{\mathbf{z}}+E\nabla^2\mathbf{u}, \qquad (1)$$

$$\tfrac{DT}{Dt}=E\nabla^2T, \qquad (2)$$

$$\nabla\cdot\mathbf{u}=0, \qquad (3)$$

where $\mathbf{u}$ is the velocity field, T the temperature, and p the pressure. The dimensionless parameters

$$E=\tfrac{\nu}{2\Omega d^2}, \quad Ra=\tfrac{g\alpha\Delta T d^3}{\nu\kappa}, \quad \sigma=\tfrac{\nu}{\kappa}, \qquad (4)$$

are the Ekman, Rayleigh and Prandtl numbers, measuring the importance of dissipation compared with the rotation rate Ω, the strength of the applied buoyancy force, and the ratio of viscous and thermal diffusion times. The variables ν and κ are, respectively, the kinematic viscosity and thermal diffusivity. Of the remaining symbols ΔT is the temperature difference imposed across the layer while g is the acceleration due to gravity and α the coefficient of thermal expansion.

In the following we assume that the rotation rate is large in the sense that $E\ll1$. Although this requirement says nothing about the local Rossby number Ro on the scales of interest ($Ro\equiv U/2\Omega L$, where U and L are, respectively, the characteristic horizontal velocity and length scale), we will be focusing on scales L for which this number is small. However, in contrast to standard geophysical applications in which the smallness of the Rossby number is due to the large scales L considered, we shall be considering small scales with correspondingly slow velocities U, and the Rossby number will be small because the rotation rate is large. Recent flow visualizations in laboratory experiments (see Fig. 5 of Sakai 1997) and numerical simulations (Julien et al. 1996) show that such a characterization is typical for turbulent rapidly rotating convection. In these investigations, tall long-lived thermal and vortical coherent structures are observed (Figure 1). These structures, whose horizontal and vertical scales are close to the dissipation scale and the layer depth, respectively, cannot be captured by reduced prescriptions such as the $2+\epsilon$–dimensional models discussed above. A complementary approach is presented here.

STREAMFUNCTION FORMULATION

In the following we employ a streamfunction formulation in order to avoid difficulties in imposing the incompressibility requirement (3) on the velocity field at each order in the asymptotic expansion. Additionally, we find that this formulation provides greater clarity in the interpretation of low Ro convection. Specifically, we set

$$\mathbf{u}:=(u,v,w)=\nabla\times\phi\hat{\mathbf{z}}+\nabla\times\nabla\times\psi\hat{\mathbf{z}}. \qquad (5)$$

Here the streamfunctions are related to the vertical velocity $w\equiv-\nabla_\perp^2\psi$ and the vertical vorticity $\zeta\equiv-\nabla_\perp^2\phi$, respectively. Horizontal mean flows $\bar{u}(z)$, $\bar{v}(z)$ (if present) require that the streamfunctions ϕ, ψ be non-periodic in (x,y). However, in the expansion that follows such flows only come in at higher order in E and hence are determined *self-consistently* by the leading order contributions to ϕ and ψ. Consequently, in the following we take both ϕ and ψ to be periodic in the horizontal and calculate the associated mean flows only *a posteriori* as necessary (*cf.* Julien & Knobloch 1997).

On taking $\hat{\mathbf{z}}\cdot\nabla\times$ and $\hat{\mathbf{z}}\cdot\nabla\times\nabla\times$ of the momentum equation, the governing equations take the form

$$\tfrac{1}{\sigma}\partial_t\nabla_\perp^2\phi-\partial_z\nabla_\perp^2\psi+\tfrac{1}{\sigma}N_\phi(\phi,\psi)=E\nabla^2\nabla_\perp^2\phi, \qquad (6)$$

$$\tfrac{1}{\sigma}\partial_t\nabla^2\nabla_\perp^2\psi+\partial_z\nabla_\perp^2\phi+\tfrac{1}{\sigma}N_\psi(\phi,\psi)=-RaE^2\nabla_\perp^2T +E\nabla^4\nabla_\perp^2\psi, \qquad (7)$$

$$\partial_tT+N_T(\phi,\psi,T)=E\nabla^2T, \qquad (8)$$

where

$$N_\phi(\phi,\psi) = (\omega\cdot\nabla)w-(\mathbf{u}\cdot\nabla)\zeta,$$
$$N_\psi(\phi,\psi) = \hat{\mathbf{z}}\cdot\nabla\times\nabla\times(\omega\times\mathbf{u}),$$

$$N_T(\phi,\psi,T) \quad = \quad \mathbf{u}\cdot\nabla T. \qquad (9)$$

The streamfunction representation of these terms can be found in Julien et al. (1998). These equations are solved for a fluid confined between impenetrable stress-free or no-slip boundaries at fixed temperatures.

REDUCED INTERIOR EQUATIONS

Anisotropic coherent structures observed in rapidly rotating convection (Sakai 1997, Julien et al. 1997, 1998) occur as an inevitable consequence of the Taylor-Proudman constraint which suppresses variation in z relative to the variation in (x,y). In the following we outline the derivation of a new class of reduced PDEs by exploiting this anisotropy (see Julien et al. 1998). Specifically we focus on horizontal scales of order $E^{\frac{1}{3}}d$ and introduce "fast" horizontal variables $x'\equiv E^{-\frac{1}{3}}x$, $y'\equiv E^{-\frac{1}{3}}y$, and use the notation $D\equiv\partial_z$ to denote derivatives with respect to the "slow" variable z. We further introduce a slow time $t'\equiv E^{\frac{1}{3}}t$ and scale the Rayleigh number according to $Ra'\equiv E^{\frac{4}{3}}Ra$. In thermal convection these are the dominant scales selected by linear theory (Chandrasekhar 1961). In contrast to the present scaling, the empirical scaling results reported for the nonlinear regime (Boubnov & Golitsyn 1986, Sakai 1997) cannot be continued into the linear regime. To retain nonlinearity in the dynamics we scale the streamfunctions according to $\phi=E\phi'$, $\psi=E^{\frac{4}{3}}\psi'$. This rescaling implies that on the length scales of interest the vertical and horizontal velocities, given by

$$\mathbf{u}=(\partial_y\phi+E^{\frac{1}{3}}\partial_x\partial_z\psi,-\partial_x\phi+E^{\frac{1}{3}}\partial_y\partial_z\psi,-\nabla_\perp^2\psi), \qquad (10)$$

are of the same order, $\mathcal{O}(E^{\frac{2}{3}})\Omega d$ in dimensional units. The local Rossby number is thus $\mathcal{O}(E^{\frac{1}{3}})$ and hence is small; i.e., even though the scales of interest are small, the flow is still rotation-dominated. Moreover, with this scaling the horizontal velocity components are in geostrophic balance at leading order. Note that the subdominant terms must be retained to satisfy incompressibility. Hence, we may interpret ϕ as a geostrophic field driven by the Taylor-Proudman constraint, and ψ as the convective field driven by the buoyancy forcing. This description is consistent with the low-Ro observations of Sakai (1997) who notes that the velocity field remains isotropic despite the appearance of Taylor-like columns in the flow field. A final step in the derivation requires splitting the temperature T into its mean and fluctuating parts: $T(x,y,z,t)\equiv\overline{T}(z)+E^{\frac{1}{3}}\theta(x,y,z,t)$. Here the overbar denotes a spatial average in the horizontal *and* a time-average. The time-averaging is an essential aspect of our decomposition, and allows us to close the problem (Julien and Knobloch 1998).

The following reduced system of equations is derived:

$$\partial_t\nabla_\perp^2\phi-J[\phi,\nabla_\perp^2\phi]-\sigma D\nabla_\perp^2\psi=\sigma\nabla_\perp^4\phi+\mathcal{O}(E^{\frac{1}{3}}), \qquad (11)$$

$$\partial_t\nabla_\perp^2\psi-J[\phi,\nabla_\perp^2\psi]+\sigma D\phi=-\sigma Ra\theta+\sigma\nabla_\perp^4\psi+\mathcal{O}(E^{\frac{1}{3}}), \qquad (12)$$

i.e., a pair of equations for the vertical velocity $w\equiv-\nabla_\perp^2\psi$ and the vertical vorticity $\zeta\equiv-\nabla_\perp^2\phi$, coupled via vertical stretching and driven by thermal buoyancy:

$$(\partial_t\theta-J[\phi,\theta]-\nabla_\perp^2\psi D\overline{T})=\nabla_\perp^2\theta+\mathcal{O}(E^{\frac{1}{3}}). \qquad (13)$$

Here $J[f,g]\equiv\partial_x f\partial_y g-\partial_y f\partial_x g$. The equations are closed using the first integral of the mean temperature equation:

$$D\overline{T}=-1-\overline{(\nabla_\perp^2\psi\,\theta-\langle\nabla_\perp^2\psi\,\theta\rangle)}+\mathcal{O}(E^{\frac{1}{3}}). \qquad (14)$$

Here the angular brackets denote a vertical average. The resulting equations describe the dynamics in the bulk, *outside* of any Ekman boundary layers required by horizontal boundaries. In the present problem such boundaries are passive (Julien and Knobloch 1998).

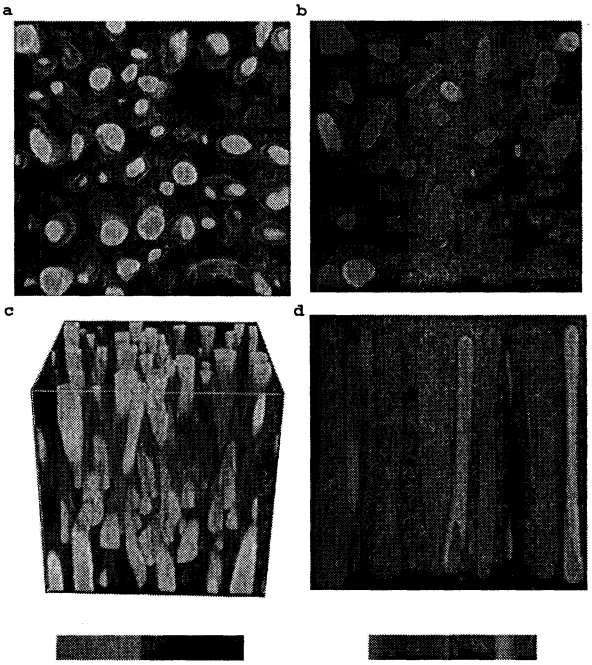

Figure 2: Visualization in λ_2 (a,c) and θ (b,d) for the reduced equations (11–14) with $Ra=20E^{-\frac{4}{3}}$; the aspect ratio is $6E^{\frac{1}{3}}\times6E^{\frac{1}{3}}\times1$ (not to scale). The flow characterization captures the coherent structures first observed in simulations of the full three-dimensional Boussinesq equations (Figure 1).

NUMERICAL RESULTS

Equations (11–14) were solved numerically (Julien et al. 1998) using a pseudo-spectral Petrov-Galerkin method in which field variables are represented with sines or cosines in the vertical and periodic Fourier modes in the horizontal. Time-stepping is via a mixed implicit/explicit 3rd-order Runge-Kutta scheme developed by Spalart et al. (1991), with the diffusion and forcing terms treated implicitly and the nonlinear and stretching terms explicitly. We set $Ra'=20$ (2.2 times critical), $\sigma=1$, and the domain width to 6 times the most unstable linear wavelength ($\lambda_\perp\approx4.8154$) in both horizontal directions. Top and

bottom boundary conditions are impenetrable/fixed temperature and side boundaries are periodic. The calculations were conducted with 64^3 spectral modes and were de-aliased in all spatial directions at each Runge-Kutta sub-timestep.

Figures 2 and 3 show fully nonlinear numerical solutions of equations (11)–(14) using only spatial averaging for the mean terms. After a very short initial transient, vortical buoyant plumes emerge and mutually advect one another laterally. The plumes are columnar, spanning the layer depth, as one expects given the Taylor-Proudman constraint. However, we reiterate that the velocity field is isotropic. These characteristics are remarkably similar to those observed in experiments by Sakai (cf. Fig. 5 of Sakai 1997). Very near the boundaries, however, sharp temperature gradients appear, as anticipated from the thermal boundary conditions. Such boundary layers are evident in $\overline{T}(z)$ in figure 3a for $z<0.1$ or $z>0.9$ where $D\overline{T}$ approaches -4.0; in comparison, at midlayer, $D\overline{T}$ is a factor of 10 smaller ($D\overline{T}\approx -0.4$). Semi-analytical investigations by Julien & Knobloch (1997, 1998), summarized below, indicate that this ratio continues to grow monotonically with increased thermal forcing. These features also resemble closely those found in numerical solutions of the full three-dimensional Boussinesq convection equations at large rotation rates (Julien et al. 1996 and Figure 1). Differences between full Boussinesq simulations (Figure 1) and the reduced equations presented here (Figure 2) are most notable near the boundaries. This is to be expected since the reduced system describes only the leading order dynamics and so is insensitive to the details of the mechanical boundary conditions. Such a system cannot capture the structure of the resulting velocity boundary layers. Finally, figure 3b shows the Nusselt number (or nondimensional heat transfer) of the time-evolving flow, and indicates that the flow develops rapidly to a near-stationary state. These solutions are representative of the possible dynamics contained within the new class of equations derived here. Moreover, in the low-Ro limit, integration over rotational timescales in this reduced prescription provides an attractive advantage compared with integration over the diffusion timescales in the full Boussinesq problem.

FULLY NONLINEAR ANALYTIC SOLUTIONS

Julien & Knobloch (1997, 1998) determine semi-analytically fully nonlinear stationary and overstable solutions to the reduced equations with certain planforms. These solutions have the form

$$\Psi=\tfrac{1}{2}\left[\Psi(Z)e^{i\omega t}h(x,y)+\Psi^*(Z)e^{-i\omega t}h^*(x,y)\right], \qquad (15)$$

where $\Psi(Z)=(\psi,\phi,\theta)$ and $h(x,y)$ is a planform function satisfying $(\nabla_\perp^2+k^2)h=0$ with normalization $\overline{h^2}=1$. Here k is the horizontal wavenumber of the planform. Admissible h yielding fully nonlinear solutions are constrained to satisfy $\partial_x h\partial_y h^*-\partial_x h^*\partial_y h=0$. In this case the Jacobians $J(\phi,\nabla_\perp^2\phi)$, $J(\phi,\nabla_\perp^2\psi)$ and $J(\phi,\theta)$ all vanish. The leading-order nonlinearity arises solely from the distortion

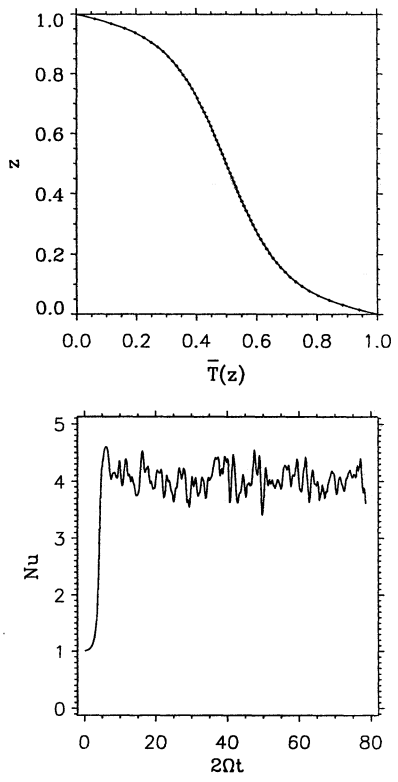

Figure 3: The unaveraged Nusselt number $Nu\equiv -D\overline{T}$ from equation (14) as a function of dimensionless time $2\Omega t$, showing rapid relaxation to a statistically stationary state.

of the horizontally averaged temperature profile. Permissible steady solutions ($\omega=0$) include rolls, squares, hexagons triangles, and patchwork quilt. Similarly, oscillatory solutions ($\omega\neq 0$) include travelling rolls and five standing-wave patterns (rolls, squares, hexagons, triangles and patchwork quilt).

Substitution of (15) into the reduced equations yields the following nonlinear eigenvalue problem for the amplitude $\psi(Z)$, frequency ω and (time-averaged) Nusselt number K:

$$D^2\psi-k^2\left(\tfrac{i\omega}{\sigma}+k^2\right)^2\psi+\frac{\left(\frac{i\omega}{\sigma}+k^2\right)(k^2-i\omega)}{k^4+\omega^2+\frac{k^6}{2}|\psi|^2}k^2 Ra\ K\ \psi=0, \qquad (16)$$

$$K^{-1}=\int_0^1 \frac{\omega^2+k^4}{\omega^2+k^4+\frac{1}{2}k^6|\psi|^2}dz. \qquad (17)$$

This problem is solved for a given Ra using a Newton-Raphson-Kantorovich algorithm (Cash and Singhal 1984), subject to the boundary conditions $\psi(1)=\psi(0)=0$. The fact that equations (16, 17) are planform-independent implies that all the permissible steady (or oscillatory) patterns are degenerate in the sense that they have identical Nusselt numbers. In Figure 4a we show the resulting Nusselt-

Rayleigh-number plots for steady and overstable convection. In Figure 4b we show the mean temperature profiles for increasing Rayleigh numbers, obtained from the relation

$$D\overline{T}=-K\left[\frac{\omega^2+k^4}{\omega^2+k^4+\frac{1}{2}k^6|\psi|^2}\right]. \qquad (18)$$

The formation of an isothermal interior bounded by thin thermal boundary layers at the top and bottom is evident. This essentially exact theory is valid for all $\mathcal{O}(E^{-\frac{4}{3}})$ Rayleigh numbers and therefore describes highly supercritical convection. The theory describes the thermal boundary layers at these Rayleigh numbers but viscous boundary layers are absent. Such thermal boundary layers must be resolved in simulations of the reduced PDEs, as discussed further elsewhere.

Important conclusions can be made from the apparent leading-order degeneracy in the above analytic solutions for steady and overstable convection. Namely, in the rapid-rotation limit the large amplitude state is characterized by a competition between a number of *computable* nearly degenerate states. Because of this near-degeneracy such competition must occur on a slow time scale. Moreover the strong influence of the Taylor-Proudman constraint implies that any instabilities lead to states that do not deviate substantially from the computable states. Consequently we expect the statistical properties of the resulting "turbulent" state to be largely independent of which of the competing states is actually present, although distinction between steady, and traveling or standing patterns is necessary. We find good quantitative agreement between the Nusselt number obtained in the simulations at $RaE^{\frac{4}{3}}=20$ and that computed from (17). Studies of two-dimensional fully nonlinear convection on an f-plane also support this picture and yield semi-analytical correlations that are in good quantitative agreement with direct numerical simulations in *three* dimensions (Hathaway and Somerville 1983).

ANELASTIC CONVECTION

The methods described above for incompressible convection can be extended to include the effects of background stratification. This effect is important for astrophysical applications and is also of interest since the up-down symmetry of the Boussinesq approximation is broken. We eliminate sound waves using the anelastic approximation (Gough 1969), focusing on dynamics on timescales long compared with the sound-travel time. The approximation requires that the basic state be adiabatic and hydrostatic. The equations describing this state, nondimensionalized with respect to temperature T_s, density ρ_s and pressure p_s at $z=0$, are

$$S_0=\text{const.}, \quad p_0=\rho_0 T_0, \qquad (19)$$

$$\frac{dp_0}{dz}=-\frac{1}{h}\left(\frac{\gamma}{\gamma-1}\right)\rho_0, \quad \frac{d}{dz}\left(K_0(z)\frac{dT_0}{dz}\right)=0, \qquad (20)$$

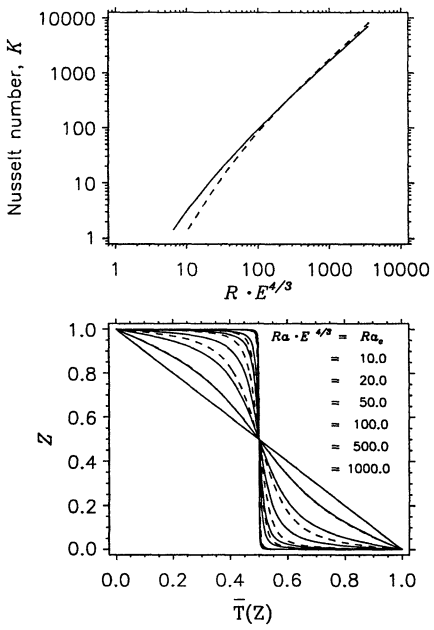

Figure 4: a) Time-averaged Nusselt number K as functions of the (scaled) Rayleigh number and b) Mean temperature profiles at various Rayleigh numbers for steady (dashed) and oscillatory (solid) convection.

where S_0 is the entropy per unit mass, $\gamma=c_p/c_v$ is the ratio of specific heats at constant pressure and volume, h is the temperature scale height and $K_0(z)$ is the (possibly depth-dependent) thermal conductivity. If $K_0=1$ the background atmosphere is found to be a polytrope with

$$T_0=\left(1-\frac{z}{h}\right), \quad \rho_0=\left(1-\frac{z}{h}\right)^m, \quad p_0=\left(1-\frac{z}{h}\right)^{m+1}, \qquad (21)$$

where $m=1/(\gamma-1)$ is the polytropic index and $h=c_pT_s/g$.

In such a stratified atmosphere convection arises as a result of buoyancy forces due to density perturbations ρ_1 of the basic state $\rho_0(z)$ assumed small compared to ρ_0 but still large enough to drive convection. Such buoyancy forces can be calculated using the *linearized* equation of state

$$\left(\frac{\gamma}{\gamma-1}\right)\frac{p_1}{p_0}=\sigma Rah\left(G\frac{\rho_1}{\rho_0}+\frac{T_1}{T_0}\right), \qquad (22)$$

and the thermodynamic relation

$$S_1=\frac{T_1}{T_0}-\frac{1}{\sigma Rah}\frac{p_1}{p_0}, \qquad (23)$$

valid for $p_1 \ll p_s$, $\rho_1 \ll \rho_s$, $T_1 \ll T_s$. Here $G=(\rho_{1s}/\rho_s)(T_s/T_{1s})$ is a nondimensional ratio of the relative density and temperature fluctuations, the subscripts 0,1 denote the basic state and the perturbation about it, and the subscript s denotes reference values. Note that this linearization is valid even for nonlinear convection.

Since the characteristic magnitude of the quantity T_1 is determined by the temperature difference ΔT imposed

across a layer of depth d we now express T_1 in units of $T_{1s} \equiv \Delta T$ and similarly for ρ_1 and p_1. Under these conditions equations (22, 23) become

$$S_1 = \frac{T_1}{T_0} + \mathcal{O}(E^{\frac{4}{3}}), \qquad G\frac{\rho_1}{\rho_0} + \frac{T_1}{T_0} = \mathcal{O}(E^{\frac{4}{3}}) \tag{24}$$

and the pressure perturbation p_1 therefore does not contribute to the equation of state at leading order.

The anelastic equations describing these motions are

$$\rho_0 \frac{D\mathbf{u}}{Dt} + \hat{\mathbf{z}} \times \rho_0 \mathbf{u} = -\nabla p_1 - \sigma Ra G E^2 \rho_1 \hat{\mathbf{z}} + E\sigma \nabla \cdot \tau, \tag{25}$$

$$\rho_0 T_0 \frac{DS_1}{Dt} = E\nabla \cdot (K_0 \nabla) T_1 + \frac{1}{RahE} \tau \cdot \nabla \cdot \mathbf{u}, \tag{26}$$

$$\nabla \cdot (\rho_0 \mathbf{u}) = 0 \ . \tag{27}$$

Here τ denotes the viscous part of the stress tensor: $\tau_{ij} = \mu_0(z)(\partial_i u_j + \partial_j u_i - \frac{2}{3}\nabla \cdot \mathbf{u}\delta_{ij})$, where μ_0 is the (possibly depth-dependent) coefficient of dynamic viscosity.

The reduced equations are now derived by introducing the streamfunction representation

$$\rho_0 \mathbf{u} = \nabla \times \phi \hat{\mathbf{z}} + \nabla \times \nabla \times \psi \hat{\mathbf{z}} \ , \tag{28}$$

and using the anisotropic scalings suggested by the incompressible case. The reduced anelastic equations that result are

$$\partial_t \nabla_\perp^2 \phi - \frac{1}{\rho_0} J[\phi, \nabla_\perp^2 \phi] - \sigma D \nabla_\perp^2 \psi = \sigma \mu_0 \nabla_\perp^4 \phi + \mathcal{O}(E^{\frac{1}{3}}) \ , \tag{29}$$

$$\partial_t \nabla_\perp^2 \psi - \frac{1}{\rho_0} J[\phi, \nabla_\perp^2 \psi] + \sigma D \phi = -\sigma Ra \frac{\rho_0}{T_0} \theta + \sigma \mu_0 \nabla_\perp^4 \psi + \mathcal{O}(E^{\frac{1}{3}}) \ , \tag{30}$$

$$\rho_0 \partial_t \theta - J[\phi, \theta] - T_0(Z) \nabla_\perp^2 \psi D\left(\frac{\overline{T}_1}{T_0}\right) = K_0 \nabla_\perp^2 \theta + \mathcal{O}(E^{\frac{1}{3}}) \ . \tag{31}$$

Here $Ra = c_p \rho_s g \Delta T d^3 / \mu_0 K_0 T_s$. The equations are closed using the first integral of the mean temperature equation:

$$D(K_0 D\overline{T}_1) = -D(\overline{\nabla_\perp^2 \psi \theta}) + \overline{\nabla_\perp^2 \psi \theta} D(\ln T_0) + \frac{\mu_0}{Rah} \overline{\tau_\mu} \ . \tag{32}$$

The last term represents the spatial average of viscous heating. This is a lengthy function and is therefore not presented here. The incompressible reduced equations are recovered in the limit of large temperature scale height, i.e. $h \gg d$.

CONCLUSION

In this paper we have shown that reduced PDEs for incompressible and anelastic convection in the low-Rossby-number limit can be derived introducing scalings that exploit the anisotropy in the observed coherent structures. The asymptotic theory is based on a relaxation of the Taylor-Proudman constraint resulting from viscous and baroclinic effects. We find that the horizontal velocity is in geostrophic balance at leading order but the vertical motions are strongly nonhydrostatic, resulting in an isotropic velocity field. This situation is markedly different from the shallow water, quasi-geostrophic and balanced models where both geostrophic *and* hydrostatic balance holds on larger horizontal scales (Pedlosky, 1998; Gent and McWilliams 1983). Remarkably, we find that the reduced PDEs have exact fully nonlinear solutions for a selected class of horizontal planforms. This theory is likely to be relevant to both laboratory experiments and numerical simulations of the Navier-Stokes equation in the rapidly rotating limit.

ACKNOWLEDGEMENTS

This work was supported by NASA under SR&T grant NAG5-4918 (KJ&JW), the Department of Energy under Grant No. DE-FG03-95ER-25251 (EK), and CU under the CRCW grant (KJ).

REFERENCES

Babin, A. V., Mahalov, A., Nicolaenko, B. and Zhou, Y., 1997, "On the asymptotic regimes and the strongly stratified limit of rotating Boussinesq equations," *Theoret. Comput. Fluid Dynamics*, Vol. 9, p. 223.

Boubnov, B. M. and Golitsyn, G. S., 1986, "Experimental study of convective structures in rotating fluids," *J. Fluid Mech.*, Vol. 167, p. 503.

Cash, J. R. and Singhal, A., 1982, "High order method for the numerical solution of two-point boundary value problems," *B.I.T.*, Vol. 22, p. 184.

Chandrasekhar, S., 1961, *Hydrodynamic and Hydromagnetic Stability*, Oxford University Press.

Gent, P. R. and McWilliams, J., 1983, "Consistent balanced models in bounded and periodic domains," *Dyn. Atmos. Oceans.*, Vol. 7, p. 67.

Gough, D.O., 1969, "The anelastic approximation for thermal convection," *J. Atmos. Sci.*, Vol. 26, p. 448.

Jeong, J. and Hussain, F., 1995, "On the identification of a vortex," *J. Fluid Mech.*, Vol. 285, p. 69.

Julien, K. and Knobloch, E., 1997, "Fully nonlinear oscillatory convection in a rotating layer," *Phys. Fluids*, Vol. 9, p. 1906.

Julien, K. and Knobloch, E., 1998, "Strongly nonlinear convection cells in a rapidly rotating fluid layer: the tilted f-plane," *J. Fluid Mech.*, Vol. 360, p. 141.

Julien, K., Legg, S., McWilliams, J. and Werne, J., 1996, "Rapidly rotating turbulent Rayleigh-Bénard convection," *J. Fluid Mech.*, Vol. 322, p. 243.

Julien, K., Knobloch, E. and Werne, J., 1998, "A new class of equations for rotationally constrained flows," *Theoret. Comput. Fluid Dynamics*, Vol. 11, p. 251.

Majda, A. J. and Embid, P., 1998, "Averaging over fast gravity waves for geophysical flows with unbalanced initial data," *Theoret. Comput. Fluid Dynamics*, Vol. 11, p. 155.

Pedlosky, J., 1979, *Geophysical Fluid Dynamics*, Springer-Verlag.

Sakai, S., 1997, "The horizontal scale of rotating convection in the geostrophic regime," *J. Fluid Mech.*, Vol. 333, p. 85.

Spalart, P. R., Moser, R. D. and Rogers, M. M., 1991, "Spectral methods for the Navier-Stokes equations with one infinite and two periodic directions," *J. Comput. Phys.*, Vol. 96, p. 297.